Arctic Cloud Characteristics as Derived from MODIS, *CALIPSO*, and *CloudSat*

MARK AARON CHAN

NASA Goddard Space Flight Center, Greenbelt, Maryland, and Center for Engineering and Sustainable Development Research, De La Salle University, Manila, Philippines

JOSEFINO C. COMISO

NASA Goddard Space Flight Center, Greenbelt, Maryland

(Manuscript received 12 April 2012, in final form 1 November 2012)

ABSTRACT

The Moderate Resolution Imaging Spectroradiometer (MODIS), Cloud–Aerosol Lidar with Orthogonal Polarization (CALIOP), and *CloudSat* Cloud Profiling Radar (CPR) set of sensors, all in the Afternoon Constellation (A-Train), has been regarded as among the most powerful tools for characterizing the cloud cover. While providing good complementary information, the authors also observed that, at least for the Arctic region, the different sensors provide significantly different statistics about cloud cover characteristics. Data in 2007 and 2010 were analyzed, and the annual averages of cloud cover in the Arctic region were found to be 66.8%, 78.4%, and 63.3% as derived from MODIS, CALIOP, and CPR, respectively. A large disagreement between MODIS and CALIOP over sea ice and Greenland is observed, with a cloud percentage difference of 30.9% and 31.5%, respectively. In the entire Arctic, the average disagreement between MODIS and CALIOP increased from 13.1% during daytime to 26.7% during nighttime. Furthermore, the MODIS cloud mask accuracy has a high seasonal dependence, in that MODIS–CALIOP disagreement is the lowest during summertime at 10.7% and worst during winter at 28.0%. During nighttime the magnitude of the bias is higher because cloud detection is limited to the use of infrared bands. The clouds not detected by MODIS are typically low-level (top height <2 km) and high-level clouds (top height >6 km) and, especially, those that are geometrically thin (<2 km). Geometrically thin clouds (<2 km) accounted for about 95.5% of all clouds that CPR misses. As reported in a similar study, very low and thin clouds (<0.3 km) over sea ice that are detected by MODIS are sometimes not observed by CPR and misclassified by CALIOP.

1. Introduction

The Arctic has been the focus of many climate change studies because of the abrupt decline of summer ice cover (Comiso et al. 2008) and of albedo feedback effects that tend to amplify global warming signals in the region (Holland and Bitz 2003). Among the key parameters involved in such feedback is the cloud cover (Kellogg 1975). Depending on cloud and surface type, clouds shield the earth from solar radiation by reflecting the radiation back to outer space and cause a general cooling of the surface (Curry et al. 1996). Other types of clouds have a warming effect because they absorb infrared radiation from the earth's surface and reemit it back to the surface. During clear sky conditions another feedback effect takes place. Clear skies allow solar radiation to reach the surface and, if the surface is covered by snow or sea ice, much of the solar radiation is reflected back to outer space. When the surface is covered by liquid water, more solar radiation is absorbed by the surface and, depending on the persistence of clear sky, this could cause a significant warming of the surface.

The study of clouds in the Arctic is timely because of large changes that are currently being observed in the region. Among the most visible of these changes is the rapid decline of the perennial and multiyear ice cover (Comiso 2012). Following reports of a rapidly declining perennial ice cover, a dramatic drop in the perennial ice extent observed in 2007 has been attributed in part to persistently cloud-free conditions in the region during the 2007 summer period (Kay and Gettelman 2009). On

Corresponding author address: Josefino C. Comiso, NASA Goddard Space Flight Center, 8800 Greenbelt Rd., Greenbelt, MD 20771.
E-mail: josefino.c.comiso@nasa.gov

DOI: 10.1175/JCLI-D-12-00204.1

© 2013 American Meteorological Society

the contrary, variation in the vertical distribution of clouds, and not the reduction in cloud amount, was reported to have caused the significant sea ice loss in 2007 (Schweiger et al. 2008). Another study from Francis and Hunter (2006) indicate that decadal increase in summer cloud amount enhances downward longwave radiation, which in turn causes warming and therefore a reduction of the extent and thickness of sea ice cover. Currently, there is still much debate as to what factors may have driven the significant loss of sea ice in recent years and how inaccurate cloud characterization has been an obstacle to achieve a conclusive analysis. Many studies of cloud cover in the Arctic have been reported using the Advanced Very High Resolution Radiometer (AVHRR) data, but the uncertainties are large because of the inability of the sensor to accurately discriminate clouds from snow- or ice-covered areas in the region (Wang and Key 2005; Curry et al. 1996). A more recent study by Karlsson and Dybbroe (2010) showed that cloud detection capabilities of the Cloud–Aerosol Lidar with Orthogonal Polarization (CALIOP) are superior compared to AVHRR and Moderate Resolution Imaging Spectroradiometer (MODIS) using matchups over the Arctic. The performance of AVHRR and MODIS is observed to be worse in December when they are able to detect only 44.41% and 63.92%, respectively, of clouds that are detected by CALIOP. Furthermore, Liu et al. (2010) found that MODIS cloud amount (but not CALIOP cloud amount) is strongly dependent on sea ice concentration, but this is in part caused by poor MODIS cloud detection capability over sea ice relative to open waters. The *Aqua*/MODIS data have provided better discrimination of clouds compared to that of AVHRR because of more channels available, but the accuracy in current cloud masking techniques has not been extensively validated. In this study, we evaluate the capability of MODIS in detecting clouds over various surface types (e.g., ice sheet and snow-covered land) prevalent in the polar regions and during nighttime and daytime conditions. The availability of near-concurrent MODIS, *CloudSat*, and CALIOP data in the afternoon constellation (A-Train) provides a unique opportunity to assess cloud cover characteristics and establish how consistently each sensor is able to detect clouds. Being active sensors, *CloudSat* and CALIOP are expected to provide independent and accurate information about the cloud cover. However, as reported in Chan and Comiso (2011), there are cases when *CloudSat* and CALIOP do not identify clouds that are clearly visible in the MODIS data. Nevertheless, we find CALIOP to provide the most accurate characterization of the cloud cover with estimated accuracy of 96.3%. This is consistent with the findings of Karlsson and Dybbroe (2010). In this study, we provide a comprehensive comparison of the capabilities of these three sensors in detecting the cloud cover in the Arctic and provide statistics on cloud cover frequencies in the region as detected by each sensor. The biases of *CloudSat* Cloud Profiling Radar (CPR) and MODIS in these statistics with respect to the CALIOP, which is used as the baseline, will also be reported and discussed. We also evaluate biases that are associated with different surfaces such as sea ice, ice sheet, and other surface types. In the end, histograms of cloud properties commonly not detected by each sensor are presented.

2. Measurements and collocation

To investigate cloud conditions over the Arctic region, we utilized data from the National Aeronautics and Space Administration Earth Observing System (EOS) A-Train (Stephens et al. 2002), where a diverse suite of active and passive sensors provides near-coincident measurement of clouds and surface characteristics. Our analysis focuses on the Arctic cloud cover as determined by key cloud sensors *Aqua*/MODIS, CPR, and CALIOP and with ancillary information on sea ice from AMSR-E. In the following sections, we briefly describe these instruments and their respective retrieval algorithm.

a. MODIS

MODIS is an imaging radiometer that measures radiances at 36 wavelengths with center wavelengths ranging from the visible to thermal infrared (0.413–14.235 μm) and spatial resolution from 250 m to 1 km. Having a scan angle of $\pm 55°$ at an orbit of 705 km, it achieves swath dimensions of 2330 km (cross track) by 10 km (along track at nadir) for every scan. One of its advantages is its high spatial resolution that provides larger statistics and a more comprehensive cloud map compared to that of active sensors. The MODIS cloud detection algorithm (Ackerman et al. 1998; Frey et al. 2008) uses a fuzzy-logic scheme to quantify whether a spectral test categorizes a particular field of view (FOV) to be confident cloudy, probably cloudy, probably clear, or confident clear. MODIS geolocation, cloud mask results, and cloud properties datasets are from MYD03 collection 5, MYD35_L2 collection 5, and MYD06_L2 collection 5.1, respectively. Previous studies indicate that over the Arctic the fractional agreement on cloud determination between MODIS and CALIOP is at 91% in August 2007 and is worse at 72% in February 2007 (Holz et al. 2008). This highlights the high dependence of the MODIS cloud detection algorithm on the visible channels and that cloud detection during the polar night

remains challenging with only the passive infrared approach. Results from Holz et al. (2008) may have indicated the influence of solar illumination on the performance of the MODIS cloud mask algorithm; however, the data volume utilized is only one month and effects of various surface types are not explored.

b. CloudSat

The cloud profiling radar on board *CloudSat* approximately trails the *Aqua* satellite by an average of about 60 s. It is a 94-GHz near-nadir-looking radar that measures the return power backscattered by clouds as a function of distance to the radar. Operating at a much shorter wavelength than typical weather radars, it is more sensitive to smaller cloud particles. A single CPR profile has a footprint of approximately 1.3 km across track and 1.7 km along track with a vertical resolution of 500 m: with 60 vertical data bins this creates a 30-km vertical data window. The CPR cloud detection algorithm (Marchand et al. 2008) differentiates radar return power that is due to scattering by any atmospheric particles (particularly clouds) from those that contain only noise. In this study, we employed the *CloudSat* standard cloud product, 2B-GEOPROF R04 (Marchand et al. 2008), that contains cloud mask results with values from 0 to 40 assigned to each vertical bin. Mask values of 20, 30, and 40 indicate considerable echo with high confidence of hydrometeor presence with very low false detection rates of only 5%, 4.3%, and 0.6%, respectively. On the contrary, very weak echoes with mask values from 6 to 10 signify cloud presence using along-track averaging. These weak echoes are mired with a very high false detection rate of 44% and are therefore considered not cloudy. In general, *CloudSat* is able to detect most clouds consistently, even for different surface types and conditions (e.g., day/night), but several issues persist such as nondetection of high thin cirrus, altocumulus, and continental stratus, as they are below the minimum detectable signal (Marchand et al. 2008). Moreover, due to strong surface clutter, CPR sensitivities within 1 km above the surface are limited, to the extent that backscatters from the lowest 500 m do not provide useful data.

c. CALIOP

CALIOP is an active sensor onboard *Cloud–Aerosol Lidar and Infrared Pathfinder Satellite Observations* (*CALIPSO*) that trails *CloudSat* by approximately 15 s. It is a near-nadir-viewing, polarization-sensitive, elastic backscatter lidar that uses a pumped neodymium-doped yttrium aluminum garnet (Nd:YAG) laser transmitting at dual wavelengths of 1063 nm and 532 nm. The two receivers for the 532-nm channels retrieve the degree of linear depolarization of the return signal, which has both perpendicular and parallel polarization components of the signal originating from the laser transmitter. The combination of total backscatter radiation measured at 1063 nm and the degree of linear depolarization at 532 nm are used to discriminate between clouds and aerosols (Liu et al. 2009). The lidar surface footprint is 333 m for both cross track and along track and has a vertical resolution of 30 m at altitudes below 8.2 km. For the cloud cover analysis, the CALIOP Vertical Feature Mask (VFM) version 3.01 is used and the data product provided feature classification within a vertical profile. There are six features identified: clear air, cloud, aerosols, stratospheric feature, surface, and subsurface. The 2B-GEOPROF-lidar R04 is a collocated product of CPR and CALIOP that provides information on the degree of cloud cover as determined by CALIOP within a radar vertical bin (cloud fraction) and it also provides a more accurate characterization of cloud-top/cloud-base heights, number of layers, and geometrical thickness.

d. AMSR-E

The Advanced Microwave Scanning Radiometer for EOS (AMSR-E) is a dual-polarized passive microwave radiometer onboard *Aqua*. It measures microwave radiation at six different frequencies from 6.9 to 89.0 GHz with the horizontal and vertical polarized components measured at each frequency. The retrieval of sea ice concentration is achieved using the Bootstrap sea ice algorithm (Comiso et al. 2003) that enables the discrimination of different mixtures of ice cover from 100% concentration sea ice to 0% (or open water). We used the AMSR-E/*Aqua* level 3 gridded product at 12.5-km spatial resolution that provides a daily averaged sea ice concentration of the Arctic region. Information about the sea ice concentration allows us to assess the changes in cloud detection performance of each of the sensors when clouds are over different sea ice concentration conditions.

e. Methodology

To evaluate cloud cover over the Arctic region, we have created a 50 km by 50 km grid on a polar stereographic projection with the true scale located at 70°N latitude using a Hughes ellipsoid. The orbital data from MODIS, CPR, and CALIOP were accumulated on each grid cell to build a monthly average cloud fraction. Nadir-looking sensors such as CPR and CALIOP have limited spatial coverage compared to an imager such as MODIS. Based on analysis of frequency distribution, it was determined that, for a reasonable statistical accuracy, the number of data points in a grid cell should be at least 90 for CPR and 450 for CALIOP. This limits

our coverage of CPR and CALIOP data to latitudes greater than or equal to 70°N. Furthermore, CPR and CALIOP, having an inclination angle of about 98.14°, have no data points above 82.5°N. Thus, monthly cloud cover values will be computed from 70° to 82.5°N. ASMR-E provided daily sea ice concentration data, and these were averaged (maintaining spatial resolution) to form a monthly mean sea ice concentration map. Sea ice edge contours are overlaid onto the cloud map to offer insights into the interrelationship between sea ice and clouds. In this study, we opted to use the MODIS cloud mask flag probably clear/probably cloudy breakpoint for cloudy and clear decision. Thus, we assign the probably clear flag to clear and, similarly, probably cloudy as cloudy. This will provide more realistic cloud cover statistics over open waters. For CALIOP, cloud features having a feature quality assurance flag of 3 (high confidence) are utilized. For CPR, cloud mask values having very low false alarm rates from 20 to 40 are employed. Finally, difference maps between MODIS and CALIOP and CPR and CALIOP are created. This was calculated only on grid cells having CALIOP or CPR data. CALIOP was chosen to be the baseline for comparison since it is the most reliable of the three cloud detection sensors and is very sensitive to the presence of clouds. There are, however, a few cases over Greenland where CALIOP misclassifies ice/snow surface features as near-surface clouds, and these often occur on steep downward slopes near the ice sheet edges. CALIOP statistical data in these regions of Greenland show unrealistic cloud frequency of 100%. By inspection, we established that, when the cloud thickness is less than 480 m as inferred from CALIOP, and the cloud base is adjacent to the ice sheet surface [determined from U.S. Geological Survey Global 30′ Elevation (GTOPO30) digital elevation map], these features are usually misclassified by CALIOP as cloudy. In this study, such features were regarded as surface features and classified as cloud free unless a cloud cover was detected above it. Such modification is justified since CALIOP finds a cloud base below the ice sheet surface. The results show more realistic statistical cloud cover values in these locations.

Combining 2B-GEOPROF and 2B-GEOPROF-lidar to produce a combined CALIOP and CPR cloud mask collocates CALIOP and CPR. The CALIOP mask is translated as a cloud fraction within a CPR vertical profile bin since a CPR footprint can overlap with about five CALIOP profiles. A cloud fraction of 100% is considered to be cloudy and 0% is clear sky for CALIOP. Intermediate values of cloud fractions (about 5% of the total data) are used in the calculation of cloud fraction but are not used in the pixel-by-pixel comparison to have confidence that MODIS is actually viewing a clear or cloudy region. The collocation of CALIOP and CPR with MODIS is a more tedious task because the parallax effect must be accounted for, as described by Holz et al. (2008) and Wang et al. (2011). This is because CALIOP and CPR do not follow the nadir flight track of *Aqua*; thus, MODIS will have a certain viewing angle when it looks into a particular scene. The surface location of a cloud as viewed by nadir-looking sensors is the surface directly below the cloud, but the surface location of a cloud as viewed by MODIS may be a few kilometers away (e.g., typically 2–3 km when cloud is located at about 10 km above the surface over the polar regions). The shift is larger when clouds are at a higher altitude. This offset must be determined to identify which MODIS FOVs are actually observing the clouds detected by CALIOP and CPR. To correct for the parallax effect, cloud-top height from 2B-GEOPROF-lidar is used in conjunction with the MODIS scan zenith and azimuth angles to determine the displacement vector. Thus, the collocation process between MODIS and CALIOP/CPR is a two-step process for a cloudy scene. The first step is to find the nearest MODIS geolocation with the CALIOP/CPR footprint and then correct for the parallax effect by applying the displacement vector to the MODIS geolocation. The parallax-corrected collocation data are then used for the statistics.

3. Results

Comparative analysis is done using coincident MODIS, CALIOP, and CPR cloud cover data that were compiled as discussed in the previous section. In the following section, we present the results of analysis of orbital data, as in Chan and Comiso (2011), to illustrate some of the most common instances of discrepancy in the cloud cover inferred from the various instruments. This is followed by a discussion of cloud cover statistics as determined by the three sensors and some insights into the discrepancies in the results.

a. Discrepancies in cloud detection for different surface types

Figures 1a and 1b show a visible image and cloud mask results from MODIS over a sea ice region in the Arctic Ocean at 1420 UTC 16 April 2010. A solid line drawn on each of the images indicates the CALIOP and CPR tracks. The visible image shows cloudiness along the track, with cloud streaks from −140° to −130°E and −125° to −90°E (labeled A), and a cloud feature is apparent from −78° to −54°E. The MODIS cloud mask (Fig. 1b) reveals a generally cloudy scene, but an extensive cloud feature near the label A in Fig. 1a was not determined as cloudy in Fig. 1b. CALIOP and CPR

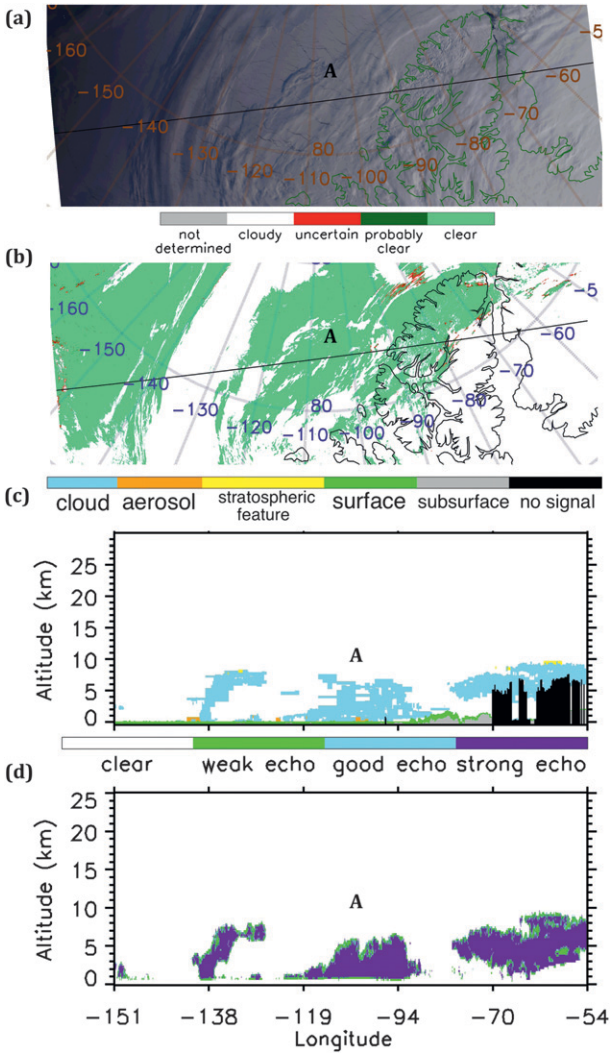

FIG. 1. (a) MODIS visible image and (b) cloud mask results with (c) CALIOP and (d) CPR vertical feature profiles over Arctic sea ice. Data are from 1420 UTC 16 Apr 2010.

vertical profiles are shown in Figs. 1c and 1d, respectively, and they indicate consistency with Fig. 1a, showing the three distinct cloud features situated at about −138°E, −105°E (labeled A), and −60°E. The cloud in A, which is obviously misrepresented by the MODIS cloud mask, is a near-surface cloud with a geometrical thickness of about 6 km (see Figs. 1c,d). As inferred from the CALIOP and CPR cloud phase product (not shown), it is a mixed-phase cloud predominantly made of ice particles in its upper 3–4-km portion with liquid droplets at the lower portion of the cloud (may not be common). In addition, it has a very low optical thickness and is basically transparent, as manifested by the ability to visually detect leads underneath it in the visible image. The MODIS spectral tests applied (Frey et al. 2008) are the 6.7-μm, 1.38-μm, the 11 − 12 μm brightness temperature difference (BTD), and 11 − 3.9-μm BTD; all of these tests, even the visible reflectance test, are unable to detect the aforementioned cloud in region A. The inability of the MODIS mask to detect this cloud is associated with the low optical depth (minimal contrast in the visible test) and comparable infrared signature with the underlying sea ice.

A case of MODIS overestimating cloud cover is presented in Fig. 2. The visible image and mask results over the Laptev Sea are shown in Figs. 2a and 2b. The visible image denotes a wispy cloud feature at 110°E, and this cloud cover is further confirmed by the mask results and vertical feature profiles from CALIOP and CPR in Fig. 2c and 2d. A stark difference is the apparent cloud cover region, labeled A, as determined by the MODIS cloud mask. Region A in the visible image does not contain any obvious cloud patterns but it has pronounced leads that are evident in the sea ice region. The CALIOP and CPR cloud data reveal that, contrary to the MODIS cloud mask, region A does not contain any major cloud feature. Furthermore, the linear patterns identified as clouds in region A by the MODIS cloud mask resemble those of the leads present in the visible image. Spectral tests that caused this particular misclassification are the 11-μm, surface temperature, 0.87-μm, 0.87 μm/0.66 μm ratio, and 1.38-μm tests. On the contrary, the BTD 11–12-μm and 8.6–11-μm tests, as well as the 6.7-μm test, confirm clear sky conditions. However, owing to the MODIS cloud mask algorithm's clear sky conservative scheme, it takes only one test that indicates cloudiness to influence the final cloud mask result to be cloudy. This is typically the case when MODIS misidentifies clear sky over sea ice or leads as cloudy regions.

Figures 3a and 3b show a MODIS visible image and cloud mask result for a different type of surface, this time over the Greenland ice sheet and Ellesmere Island at 1405 UTC 18 April 2010. For most MODIS images, it is a difficult task to visually observe cloud cover on snow-covered surfaces, and it is easier when clouds are marked with shadows. In Fig. 3b, the MODIS cloud mask contains a relatively clear scene over northern Greenland. However, CALIOP and CPR indicate otherwise, as illustrated in Figs. 3c and 3d. A vast cloud cover actually persists over the ice sheet from −65° to −37°E (labeled A). It is inferred from CALIOP data that this cloud feature is an ice cloud having a base adjacent to the surface of the ice sheet. The MODIS cloud mask algorithm used the polar day processing path, and all of the infrared tests applied, namely, the 6.7-μm, BTD 11–12-μm, and BTD 11–3.9-μm tests, did not detect cloud A. On the other hand, the visible-reflectance 1.38-μm test was not employed because of the high

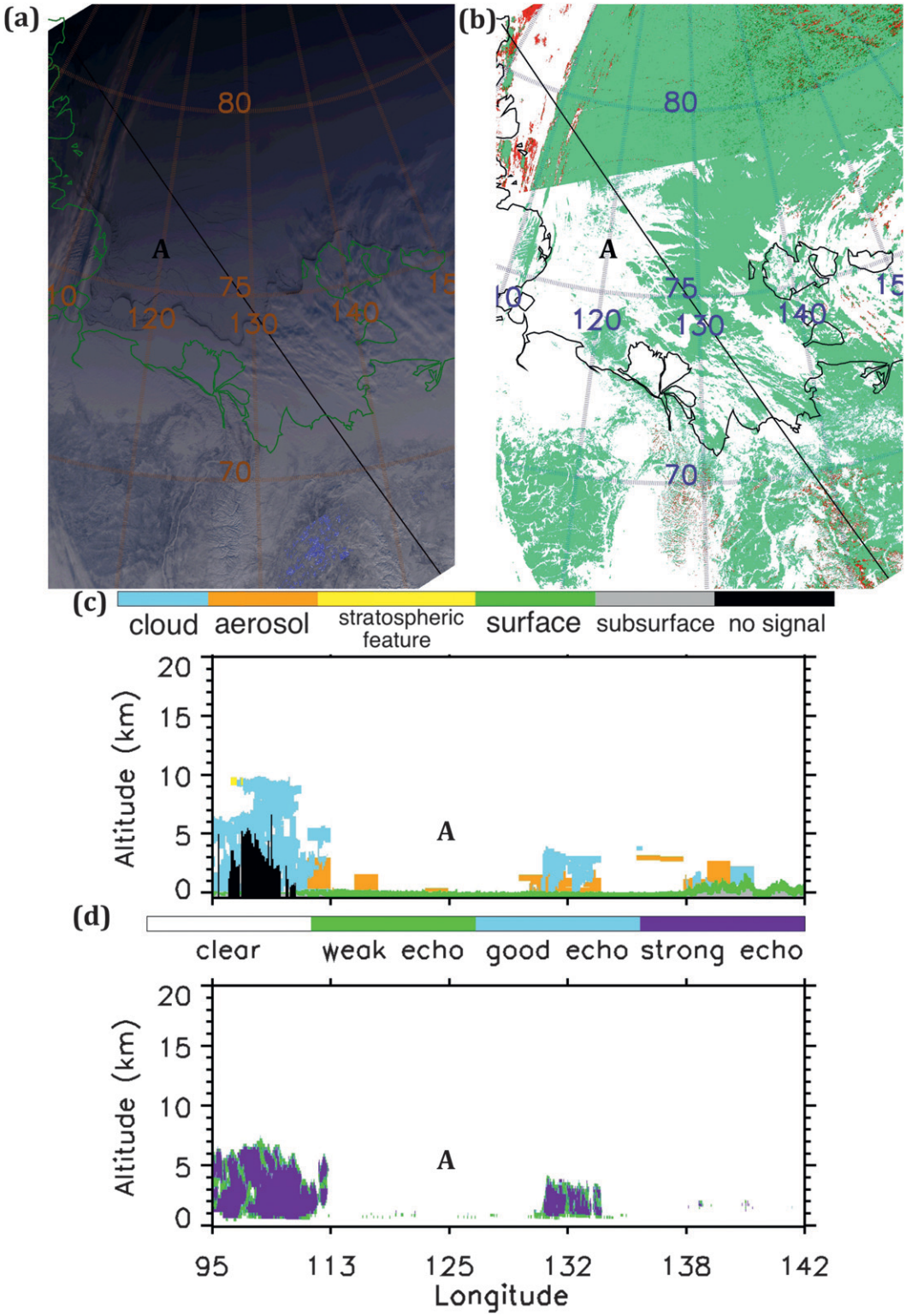

FIG. 2. (a) MODIS visible image and (b) cloud mask results with (c) CALIOP and (d) CPR vertical cloud profiles over Laptev Sea, where MODIS misidentifies sea ice as clouds. Data are from 0255 UTC 5 Mar 2007.

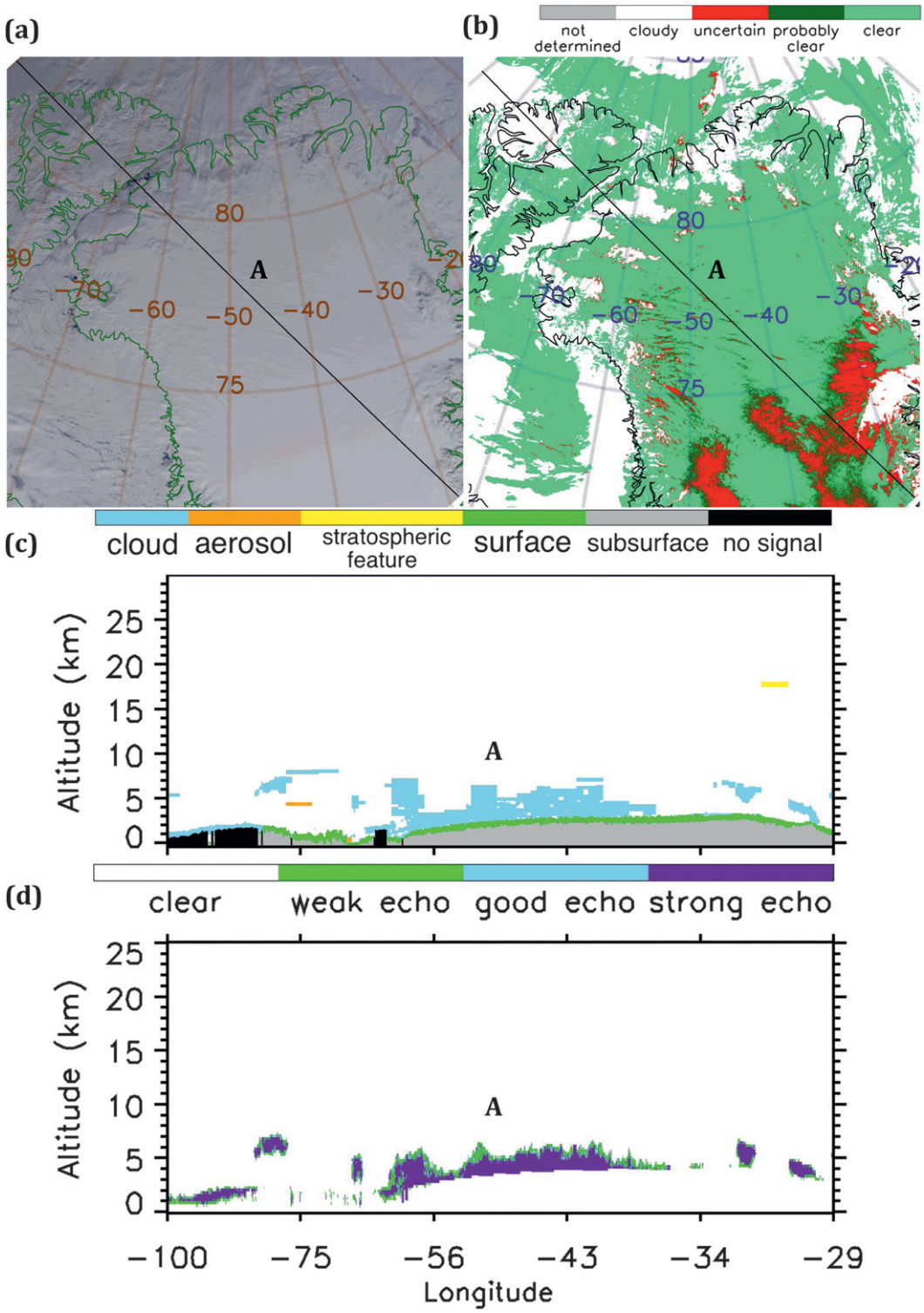

FIG. 3. (a) MODIS visible image and (b) cloud mask results with (c) CALIOP and (d) CPR vertical feature profiles over Greenland and Ellesmere Island. Data are from 1405 UTC 18 Apr 2010.

surface elevation of the ice sheet. Again, because of the proximity of the cloud to the surface and the availability of only the infrared channels, it was difficult to identify the cloud feature. Over Ellesmere Island, the vertical profiles, as observed by CALIOP and CPR from −100° to −80°E, show a stratus cloud at altitudes of 2 km. This time, the MODIS cloud mask was able to detect this liquid cloud because it has a relatively high optical thickness of more than 10.

When snow-covered regions have a reflectivity comparable to that of clouds, they are often misclassified by MODIS as a cloudy scene instead of clear sky. Figure 4a shows a MODIS visible image indicating a relatively clear scene over Greenland with some clouds located over adjacent open waters. Again, the MODIS cloud mask results provide a different depiction of cloud cover, as shown in Fig. 4b. It indicates a vast cloud feature over the central part of Greenland, labeled A. Collocated data from CALIOP and CPR are presented in Figs. 4c and 4d, and it is apparent that it is cloud-free over the entire CALIOP and CPR tracks, including the region labeled A. In this case, the MODIS cloud mask is again in disagreement with the MODIS visible data and with the CALIOP and CPR data, and the spectral tests responsible for this particular misclassification are the visible reflectance test at 0.66 μm and reflectance ratio test of 0.87 and 0.66 μm.

The inability of the MODIS cloud mask to accurately detect the presence of clouds usually gets exacerbated during nighttime, as also reported by Liu et al. (2010). A visible image and a color-coded image of brightness temperatures at 11 μm over the Laptev Sea at 2210 UTC 19 March 2010 are shown in Fig. 5a and 5b. The visible image in Fig. 5a depicts the transition between night (section labeled A) and day (section labeled B), while the thermal image in Fig. 5b provides information over both the day and night side of the scene. The day side part of the visible image captures the presence of cyclonic clouds having relatively warmer temperatures than the sea ice surface. The MODIS cloud mask product is presented in Fig. 5c and it shows a clear-cut difference in the accuracy between day side retrievals (B section) versus nightside retrievals (A section). The obvious cloudy region at B and the abrupt cloud-free region at A in Fig. 5c are delineated by a marked change depicted by the slanting line at 150°E. CALIOP and CPR data show, in Figs. 5d and 5e, a continuous band of ascending clouds from 165°E to 115°E, indicating proper retrieval in B but not in A (the nighttime region). Over the nighttime side, the polar night processing path was executed by the MODIS cloud mask algorithm, and all of the infrared tests—namely, the BTD 3.9 – 12-μm, BT 6.7-μm, BTD 11 − 3.9-μm, and BTD 7.3 − 11-μm tests—are not able to detect the nighttime section of the cloud. This shows a higher accuracy in the retrieval during daytime, when the visible channels of MODIS can be used for cloud detection, than during nighttime. Interestingly, CPR does not detect the layer of geometrically thin cirrus (~10 km high) at B. Although this particular limitation of CPR is well described by Marchand et al. (2008), the study did not indicate how frequently this occurs. A quantification of the statistics will be presented in a later section for the Arctic region. In Figs. 5b and 5c, some lead features (in region C) are apparent showing warmer thermal signatures than the surrounding sea ice. In this region, the MODIS mask indicates that it is probably clear.

We have shown cases where the MODIS mask does not provide the correct identification of the cloud cover. In a previous report, we have also shown that CALIOP and CPR are not able to detect some low-level marine clouds with geometrical thickness less than 1 km (Chan and Comiso 2011). To demonstrate that this case is not confined to marine clouds only, we present in Figs. 6a and 6b a similar case but in a sea-ice-covered region. Figures 6a and 6b show an approximately round-shaped cloud, labeled A, between −120° and −140°E. Coincident CALIOP and CPR track data, as shown in Figs. 6c and 6d, indicate that the region labeled as A is identified by both sensors as cloud free. As retrieved from MODIS data, cloud A has an approximate maximum optical thickness of 8 and top height of 2.4 km. These characteristics are consistent with those of the cases reported by Chan and Comiso (2011). There is, however, one major difference in that the reflectance as observed by the MODIS visible channel did not change much from the cloud-free to the cloud-covered area. The top of atmosphere (TOA) reflectances of cloud-free sea ice and the cloud feature over sea ice in A are very similar and are both about 20%. The MODIS cloud mask algorithm used a daytime-ocean processing path (i.e., ice free) despite the obvious sea ice cover, and this is because the high Normalized Difference Snow Index (NDSI) indicates that region A is not a snow/ice-covered surface. Subsequently, the visible test using the 0.87-μm channel is the only test that was able to detect this particular cloud feature. This is expected since clouds over a sea ice surface typically exceed the TOA reflectance threshold of 6.5% (for open waters). In this case, the spectral tests for polar surfaces would have identified the feature in A as no cloud. It was detected as cloud only because the NDSI incorrectly determined region A as a snow/ice-free surface. A closer look into the CALIOP cloud mask reveals that there is an apparent topographical augmentation of about 270 m between −126° and −136°E, which is exactly at the location of the cloud in A. Because of a very strong backscatter of about

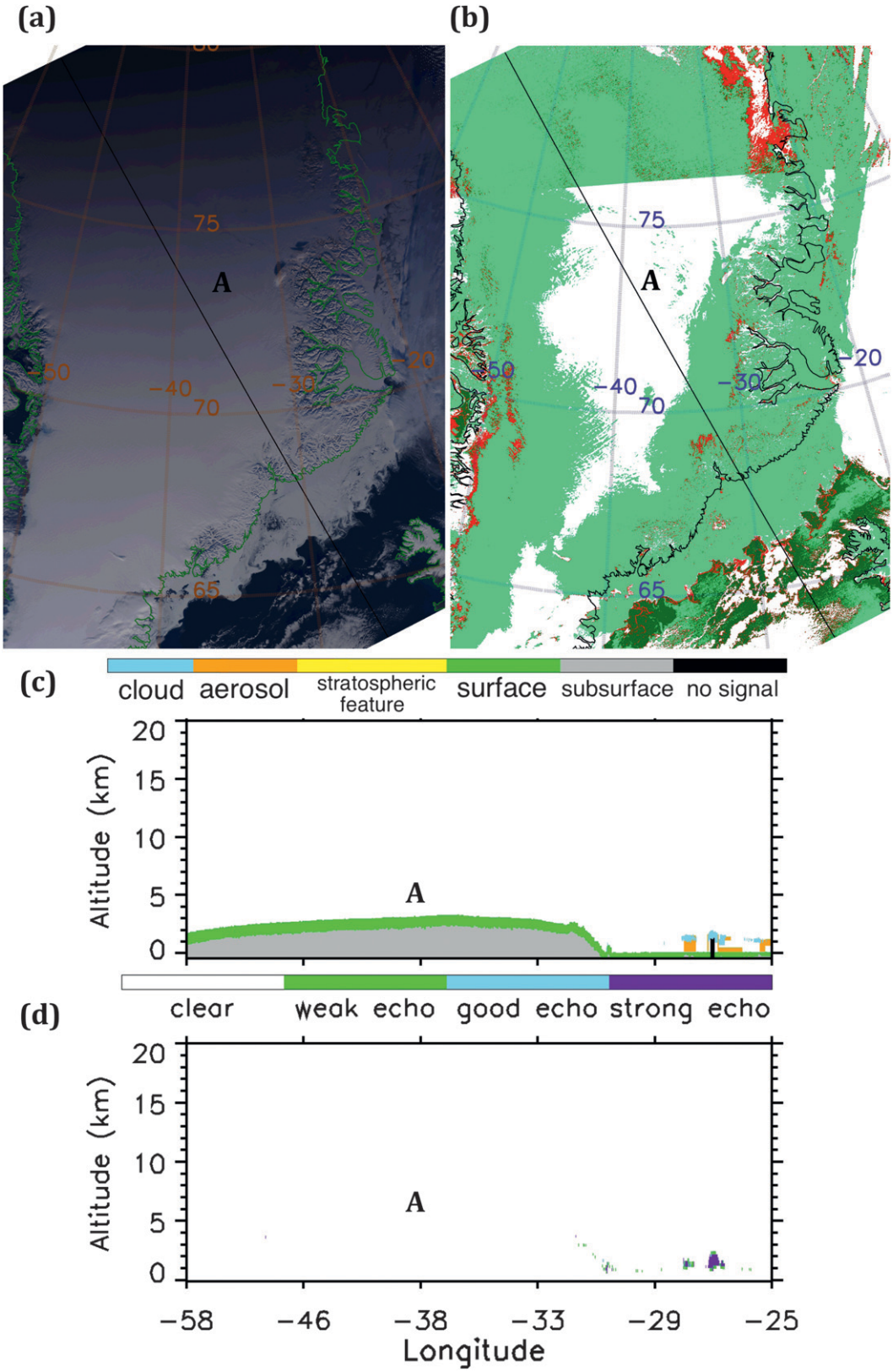

FIG. 4. (a) MODIS visible image and (b) cloud mask results with (c) CALIOP and (d) CPR vertical cloud profiles over Greenland, where MODIS misidentifies a large portion of the ice sheet as clouds. Data are from 1420 UTC 26 Feb 2007.

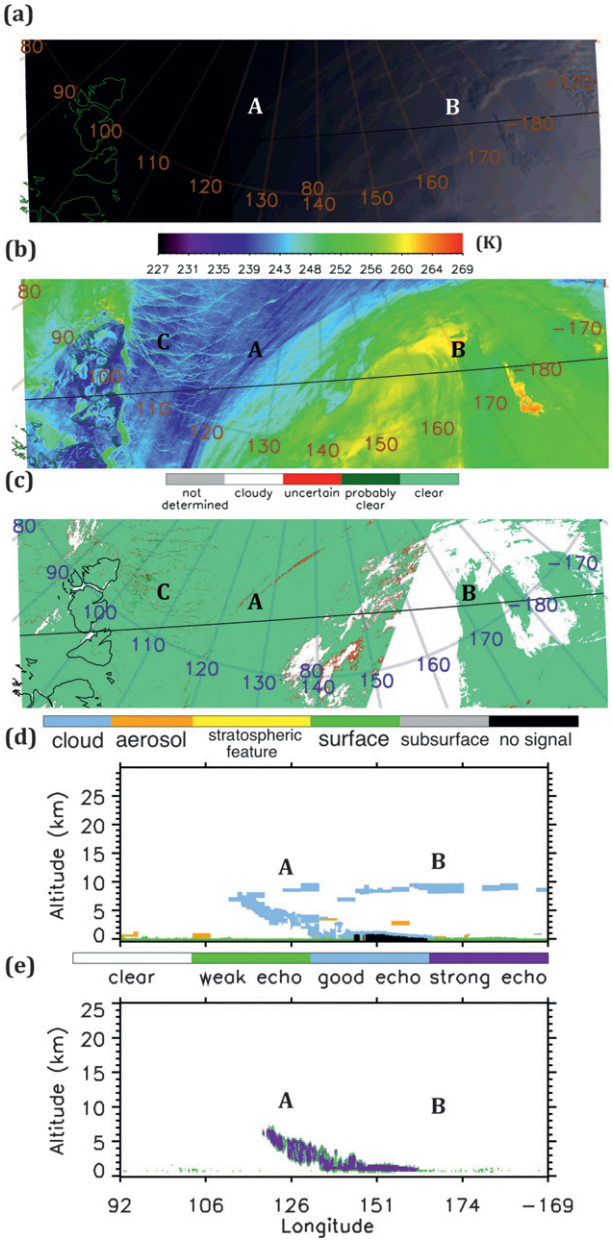

FIG. 5. (a) MODIS visible image, (b) thermal image (brightness temperature at 11 μm), and (c) cloud mask results with (d) CALIOP and (e) CPR vertical feature profiles over Laptev Sea during dayside and nightside transition. Data are from 2210 UTC 19 Mar 2010.

0.1 km^{-1} sr^{-1}, a moderate depolarization ratio of 0.4 from the cloud in A coupled with a geometrically thin feature, and a cloud base close to the surface, these types of clouds are usually misclassified by CALIOP as surface features. According to the statistics from Hu et al. (2009), these low-lying clouds (<0.3 km) with said properties are most likely to be liquid clouds. This may also be the case for the misclassified marine clouds (Chan and Comiso 2011). With the exception of these types of clouds, CALIOP

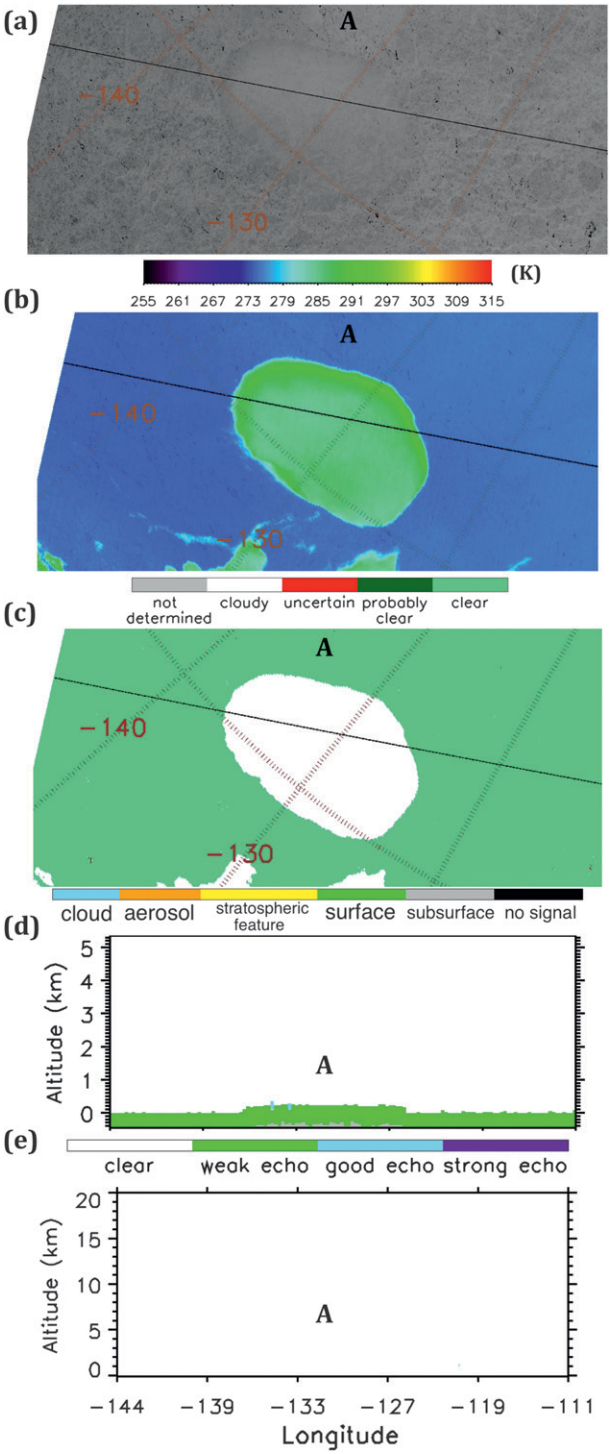

FIG. 6. (a) MODIS visible image at 0.66 μm (gray scale), (b) MODIS brightness temperature at 3.75 μm (rainbow scale), and (c) cloud mask results with (d) CALIOP and (e) CPR vertical feature profiles over sea ice on Beaufort Sea. Data are from 1425 UTC 26 Jun 2010.

provides the most dependable information about cloud presence: hence, these data will be used as the baseline for comparison in the following sections.

b. Arctic cloud cover in winter and late summer

To get an idea how the large-scale distribution of the Arctic cloud cover changes from winter to summer, cloud cover data from all three sensors were processed for the months of February and September 2007, which are the months of maximum and minimum sea ice extents, respectively. This also allowed us to investigate the cloud detection capabilities of MODIS, CALIOP, and CPR over different surface conditions and gain insights into the detection errors over these surfaces during different seasons. The average monthly cloud fraction for February 2007, as observed by CALIOP, is presented in Fig. 7a, and it appears that over the region of coverage (70°–82.5°N) the cloud fraction is generally between 50% and 100%, averaging about 71.2%. The corresponding sea ice concentration map is presented in Fig. 7b; it appears that clouds are more dominant in the open water regions compared to the ice-covered regions of the Arctic Ocean. Cloud cover in sea ice regions (concentrations ≥50%) is 69.5% and for open water it is as high as 90.0%. This difference is caused in part by the high moisture flux from open water, which is conducive for cloud formation.

A larger contrast in the cloud fraction is evident in the MODIS cloud fraction data shown in Fig. 7c, which indicates an average cloud percentage of 91.5% in the open ocean and 45.7% in the sea-ice-covered regions. Unusually low cloud fraction is evident over sea-ice-covered areas in the Beaufort, Chukchi, and Laptev Seas. The distinctly large disparity in cloud cover values over sea ice and open water is intriguing, and the sea ice edge, as indicated in Fig. 7b, seems to completely delineate cloudless regions from cloudy regions in the MODIS mask. This is in agreement with the observation of Liu et al. (2010) that the MODIS cloud amount has a negative bias at higher sea ice concentrations. It is apparent, however, that the monthly averages of cloud fraction from MODIS are strongly in disagreement with those from CALIOP. To quantify the discrepancy, a difference map between MODIS and CALIOP is presented in Fig. 7d; CALIOP provides higher percentages of clouds in the sea-ice-covered areas and slightly lower percentages in open water areas than MODIS. Overall, MODIS cloud amount over the Arctic study region is 53.1%, which is the lowest inferred from the three sensors.

The cloud cover as observed by CPR (Fig. 7e) is shown to be correlated with the CALIOP data, averaging 56.5% over sea ice, relatively low over Greenland at 38.7%, and moderately high over open waters at about 80.5%. Over the entire study region, the average cloud fraction from CPR data is 57.1%. It is apparent that CPR detects fewer clouds for all different surface types compared to CALIOP. This is expected given the frequent occurrence of low-level clouds (<2 km) over the polar regions and the cloud detection limitations of CPR for clouds below 500 m. The difference map in Fig. 7f shows that CPR and CALIOP have slight discrepancies in cloud cover for all surfaces, except Greenland where negative values indicate underestimation of cloud amount. Compared to MODIS, CPR provides lower cloud fractions over most surface types, except for clouds over sea ice where CPR cloud fractions are 10.8% higher than those of MODIS. This suggests that the MODIS cloud detection technique over sea ice is not so reliable, as indicated previously, especially during wintertime (or nighttime) when the region is deprived of visible light. The largest disagreements on cloud cover among the three sensors occur over Greenland, suggesting the dominance of near-surface clouds in highly elevated regions. This is mainly because CPR is unable to detect clouds within 500 m above the surface and MODIS is unable to identify low-level clouds that have similar thermal infrared signatures as for the underlying ice/snow surface.

The cloud cover as observed by CALIOP in September 2007, when the record minimum in the summer ice cover was observed (Comiso et al. 2008), is presented in Fig. 8a. The corresponding ice concentration during this month is presented in Fig. 8b. The Arctic during this month exhibits a high degree of cloudiness, as revealed by CALIOP data. In the sea ice regions, the average cloud fraction is 83.2% (compared to 69.5% during February), while in the open water regions the average is about 93.8%. In Greenland the seasonal change is relatively minor with the increase from 63.3% in February to 65.8% in September yielding a net difference of 2.5%. For the Arctic region study area (70°–82.5°N), the average cloud fraction is 87.9%, representing a net increase of 16.7%. This increase is mainly due to the presence of a large area of relatively cloudy open water in the Arctic basin during the period.

The cloud cover fraction, as detected by MODIS, also indicates a very cloudy Arctic in September, as shown in Fig. 8c. The cloud amount over sea ice (ice concentrations ≥50%) of 68.2% in September is considerably higher, by 22.5%, than that in February. The average cloud fraction in September over the study area is 83.7%, which is also much higher than that in February. MODIS and CALIOP cloud fractions appear similar, but the cloud cover patterns are very different, as shown in Figs. 8a and 8c. The MODIS-retrieved cloud fractions for September have similar characteristics with the data for February: the sea ice edge (50% concentration) seamlessly separates

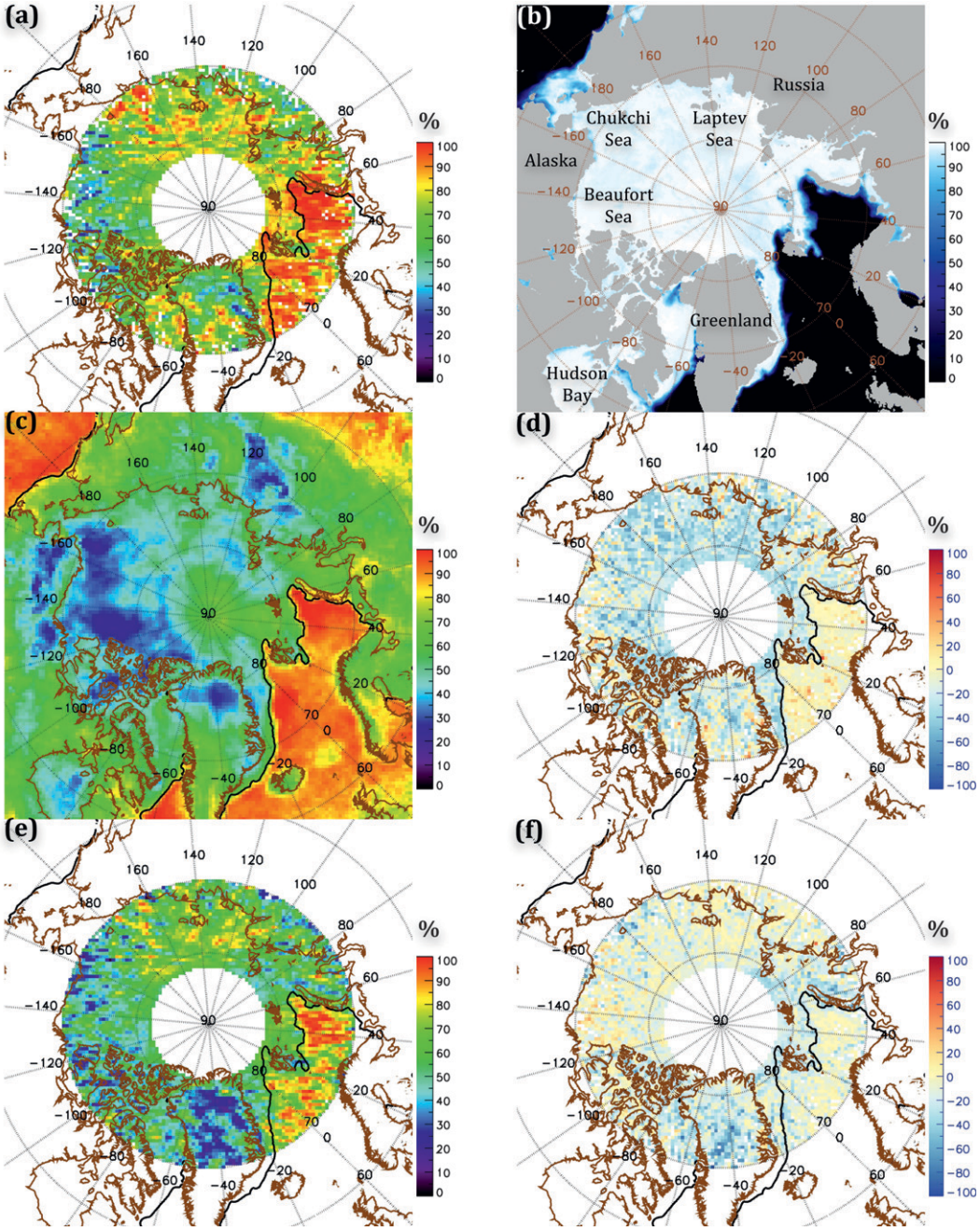

FIG. 7. Averaged monthly Arctic (a) CALIOP cloud fraction, (b) AMSR-E sea ice concentration, (c) MODIS cloud fraction, (d) MODIS minus CALIOP cloud fraction, (e) CPR cloud fraction, and (f) CPR minus CALIOP cloud fraction for February 2007.

the cloudy and cloudless regions. Kay and Gettelman (2009) also observed such a suspiciously strong spatial association of clouds with the sea ice margin. This is an indication that the MODIS cloud detection has a tendency to find higher cloud amounts over open water compared to that within the sea ice region. Over Greenland the cloud amount has substantially increased as well, from 44.7% in February to 61.8% in September. The change from February to September is much more drastic than that observed by CALIOP (i.e., from 63.3% to 65.8%). The increase in MODIS cloud fraction over Greenland represents the improvement in accuracy in MODIS cloud detection during a predominantly daylight condition, as discussed earlier. It is also evident

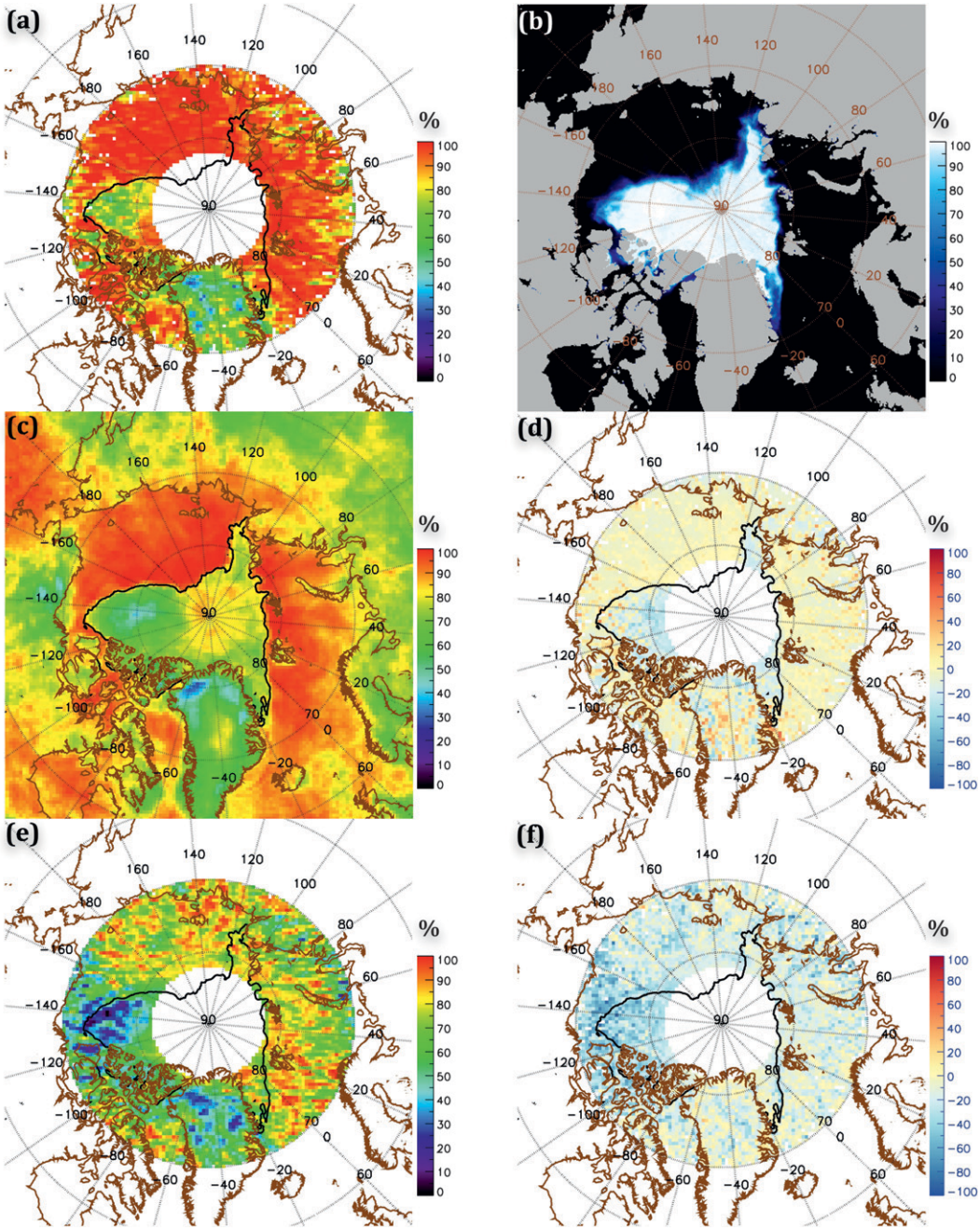

FIG. 8. As in Fig. 7, but for September 2007.

from the difference map, shown in Fig. 8d, that there is a dominance of positive values in cloud amount over open water and negative values over sea ice. This observation is similar to the case in February, but the differences are not as large.

Figure 8e shows the distribution of Arctic cloud amount in September as observed by CPR, and it is evident that the cloud fraction is relatively low over the Beaufort Sea and Greenland and is higher over open water. The average cloud fraction of 68.3% for the Arctic study area from CPR is less than that from both MODIS and CALIOP. It is apparent that CPR observes fewer clouds on all surface types: 56.1% cloud fraction over sea ice, 74.8% over open water, and 55.7% over Greenland. The overall Arctic difference map shown in Fig. 8f further illustrates the large contrast, which is much higher than that for February. The larger negative differences for CPR are due to its inherent inability to

TABLE 1. Statistics of collocated MODIS, CALIOP, and CPR cloud fractions and differences for the entire year 2007 and 2010. MODIS values in parentheses are for those classified by MYD35 as confident cloudy/clear only. "Cloudy" disagreement means that CALIOP detects the cloud, but considered clear by MODIS or CPR. "Clear" disagreement means that CALIOP indicates cloud-free conditions that are cloudy for the other sensor.

	Cloud fraction			MODIS/CALIOP disagreement		CPR/CALIOP disagreement	
Arctic (60°–82°N)	MODIS	CALIOP	*CloudSat*	Cloudy	Clear	Cloudy	Clear
Total	66.8% (68.2%)	78.4%	63.3%	20.0%	19.2%	19.1%	9.7%
SIC > 90%	59.7% (58.3%)	81.1%	64.9%	30.9%	16.7%	20.1%	14.3%
SIC 10%–90%	80.2% (81.9%)	86.1%	61.2%	13.5%	38.3%	26.4%	4.5%
Open water	88.3% (97.7%)	88.1%	72.3%	3.7%	28.2%	16.8%	9.3%
Greenland	54.6% (52.9%)	73.4%	59.3%	31.5%	21.3%	18.4%	6.9%
Day	73.1% (75.3%)	78.9%	61.4%	13.1%	20.9%	20.9%	8.8%
Night	60.8% (60.7%)	77.9%	65.1%	26.7%	17.7%	17.3%	10.4%

detect some of the low-level clouds, which are frequent during summer.

We have observed large discrepancies of cloud cover fractions as inferred from CALIOP, MODIS, and CPR. In February the discrepancies are largest because MODIS underestimates cloud cover due to the lack of solar illumination and the inadequate thermal contrast between clouds and the underlying snow or ice surfaces. The discrepancies are less apparent in September, when the availability of visible light improved cloud discrimination. CPR generally underestimates cloud cover for all surface types and atmospheric conditions except in sea ice regions during winter conditions.

The cloud fractions detected by the three sensors are generally inconsistent, especially during the winter (or nighttime) period. Some improvements in the detection algorithms will minimize the differences. To be able to assess the usefulness of current products, we provide the results of a statistical analysis of collocated FOVs of CALIOP, MODIS, and CPR over a 2-yr period.

c. *Cloud cover statistics in the Arctic*

The cloud cover statistics for MODIS, CALIOP, and CPR are evaluated by using collocated data in the Arctic from all three instruments for the entire year of 2007 and 2010, and the results are presented in Table 1. About 35 million collocated pixels were analyzed, and the cloud fractions for the entire Arctic study area (60°–82.5°N) and also separately over sea ice, Greenland, and open water are presented. For the statistics and pixel-by-pixel comparison, the study area has been extended from 70°N (in the climatology) to 60°N. For completeness, statistics for day and night and for the different seasons are also presented. Table 1 also provides information about the percentage disagreement between the systems. The value for the clear or cloudy disagreement percentages is computed by counting the number of contradictory instances between MODIS or CPR against CALIOP in identifying clear or cloudy pixels (e.g., MODIS detects cloudy but CALIOP indicates clear) and is divided by the total number of clear or cloudy observations from CALIOP. The percentage will approach 100% for no agreement while a perfect agreement is 0%. The MODIS cloud fraction column consists of two values. The cloud fraction values without parenthesis are cloud fraction statistics that include probably clear (reassigned as clear) and probably cloudy (reassigned as cloudy), whereas the cloud fraction values with parenthesis include data only from confident cloudy and confident clear. Not including probably clear/cloudy data would exclude a significant fraction of the data and can cause some bias in the statistics. In particular, we get an unrealistically high percentage of 97.7% cloudiness over open water when using only data considered as confident cloudy/confident clear.

The Arctic cloud fractions as inferred from the different sensors are shown to have large discrepancies. CALIOP indicates a very cloudy Arctic with 78.4% cloud fraction, while MODIS and CPR identify fewer clouds at 66.8% and 63.3%, respectively. A relatively high disagreement between MODIS and CALIOP is also indicated, with 20.0% and 19.2% disagreement for cloudy and clear scenes, respectively. The disagreements between CPR and CALIOP are similarly high at 19%, although clear sky disagreement at 9.7% is much lower compared to that for MODIS. This signifies that cloud detection over the Arctic region remains challenging for microwave radar and spectral imager alike. As discussed in the previous section, there are cloud detection biases over various surface types, and this is especially evident for MODIS, which indicates cloud fractions are much less over sea ice and almost 90% over open waters.

For the different surface types, Greenland has the least cloud fraction value of 54.6% from MODIS, 73.4% from CALIOP, and 59.3% from CPR. It is also where the disagreement between CALIOP and MODIS is

highest with a percentage disagreement at 31.5% for cloudy pixels. The sea ice region was divided into those with sea ice concentrations (SIC) greater than 90% and those with SIC less than 90% to better understand the difference in the cloud cover between sea ice and open water. There is indeed a change in cloud amount from the marginal ice zone (10%–90% SIC) to the consolidated ice area (>90% SIC) with the fraction changing from 80.2% to 59.7% for MODIS, 86.1% to 81.1% for CALIOP, and 61.2% to 64.9% for CPR. However, all three sensors do not agree in the sign and magnitude of the cloud fraction change from marginal to consolidated sea ice regions, with MODIS data indicating a large reduction of clouds by 20.5%, while CALIOP indicates a slight 5.0% reduction and CPR shows a slight increase of 3.7%. Over consolidated sea ice regions, the cloud identification from CALIOP and MODIS disagrees by 30.9%. The percentage disagreements decrease abruptly in the marginal sea ice regions and open waters to 13.5% and 3.7%, respectively. The drastic improvement in the MODIS cloud detection of as much as 27.3% from sea ice (SIC > 90%) to open waters supports our previous analysis that MODIS severely underestimates cloud cover over sea ice, which is also consistent with the findings of Liu et al. (2010) where MODIS cloud detection hit rate is higher over open waters. As a consequence, MODIS cloud fraction appears to increase sharply from snow/sea ice–covered regions to open waters, which is evident in the MODIS Greenland and sea ice (>90%) cloud fraction values. MODIS cloud fraction over marginal sea ice zones increased sharply by 20.5% from its values over highly concentrated sea ice regions (SIC > 90%), reporting even higher values compared to that for CPR. However, the improvement in the MODIS cloud detection over marginal sea ice comes with an expense, as the disagreement with CALIOP clear sky pixel increased to 38.3%. This implies that the presence of sea ice exacerbates the false identification of clear sky as clouds. The MODIS cloud detection bias (underestimation) over sea ice causes an unrealistic distribution of clouds, especially at the marginal sea ice region. The bias would also cause inaccurate estimates of radiative and heat fluxes between the surface and the atmosphere. On the other hand, CPR cloud detection is less influenced by changes in surface type with cloudy percentage difference against CALIOP constantly above 15% for all cases. The highest percentage difference occurred over marginal sea ice regions at 26.4%; this is because of the abundance of low-level clouds (<2 km). The CPR clear sky determination has a better overall agreement with CALIOP compared to MODIS, at a much lower percentage disagreement of 9.7%. The highest disagreement for clear sky is over sea ice (SIC > 90%) at 14.3%, while the lowest is over a marginal sea ice zone (SIC 10%–90%) at only 4.5%.

To illustrate the effect of solar illumination on cloud detection, Table 1 also shows a statistic of cloud detection during night and day. Nighttime is specified by a solar zenith angle of 85° or more; conversely, daytime is when the zenith angle is less than 85°. MODIS data suggest that daytime is much cloudier than nighttime by as much as 12.3%, while CALIOP data indicate a nearly constant cloud cover with a reduction of only 1% from daytime to nighttime. Contrary to both MODIS and CALIOP, cloud cover increases from daytime to nighttime according to CPR cloud data. The large reduction in cloud cover from MODIS is erroneous (see Fig. 5), as manifested by the large percentage difference between MODIS and CALIOP. During daytime, cloud cover disagreement between MODIS and CALIOP is 13.1%, while at nighttime it is 26.7%. This result is contrary to the surprising results by Holz et al. (2008) that indicate consistent MODIS cloud detection performance during night and day over the tropics and midlatitude. This may be true, and it means that there is sufficient thermal contrast between clouds and the underlying surface over the midlatitude regions and tropics for accurate MODIS nighttime cloud detection. However, this argument does not hold over the polar regions, where visible channels are essential for the proper discrimination of clouds from the cold, snow/ice-covered surfaces—hence the MODIS cloud detection performance discrepancy between polar daytime and nighttime. On the other hand, the percentage disagreement between CPR and CALIOP is worse during daytime at 20.9% and improves to 17.3% at night. The probable reason why CPR captures more clouds during nighttime compared to daytime is that clouds tend to thicken through the night and start precipitating because of cooler temperatures, so in the process some of the undetected daytime clouds can be detected by CPR at night.

Table 2 is included to provide insights into seasonal variation of clouds and cloud detection performances. An interesting observation is that the three sensors do not seem to agree in the seasonal variation of clouds or the season for cloud cover maximum and minimum. It is encouraging that the values from CALIOP, which we used as the baseline, are generally consistent with measurements by a radar–lidar system on the ground [i.e., Atmospheric Radiation Measurement Program (ARM)]. The cloud fractions detected at Barrow, Alaska, are 68.3%, 69.3%, 82.0%, and 91.1%, respectively, for winter, spring, summer, and autumn (Dong et al. 2010). The corresponding values for CALIOP are 73.3%, 75.6%, 78.5%, and 85.5%. The seasonal variability of clouds as inferred from ARM data is consistent with CALIOP but

TABLE 2. Statistics of collocated MODIS, CALIOP, and CPR cloud fractions and differences for different seasons for the entire years of 2007 and 2010: winter (December–February) spring (March–May), summer (June–August), and autumn (September–November).

	Cloud fraction			MODIS/CALIOP disagreement		CPR/CALIOP disagreement	
Arctic (60°–82°N)	MODIS	CALIOP	*CloudSat*	Cloudy	Clear	Cloudy	Clear
			Winter				
Total	57.8%	73.3%	61.7%	28.0%	19.9%	17.7%	11.5%
SIC > 90%	48.4%	74.6%	63.1%	41.3%	18.9%	18.4%	16.1%
SIC 10%–90%	69.4%	87.0%	66.5%	25.3%	37.7%	21.8%	6.4%
Open water	89.3%	89.8%	81.7%	4.3%	32.0%	9.8%	15.7%
Greenland	62.1%	74.6%	56.2%	26.4%	33.2%	23.6%	5.6%
Day	65.0%	63.4%	55.1%	12.2%	25.9%	16.0%	9.8%
Night	56.7%	74.8%	62.7%	29.9%	18.6%	17.9%	11.8%
			Spring				
Total	60.8%	75.6%	62.2%	24.8%	15.0%	18.3%	10.3%
SIC > 90%	60.7%	80.9%	65.9%	29.1%	12.3%	18.9%	15.2%
SIC 10%–90%	80.3%	85.2%	61.4%	12.0%	34.0%	25.7%	5.1%
Open water	87.3%	87.9%	75.8%	3.9%	21.7%	13.3%	11.4%
Greenland	42.9%	69.7%	56.8%	44.3%	17.9%	17.8%	7.0%
Day	66.1%	77.4%	63.3%	19.9%	16.7%	18.0%	10.6%
Night	50.3%	72.2%	59.9%	34.9%	12.4%	18.8%	9.8%
			Summer				
Total	74.9%	78.5%	57.3%	10.7%	22.1%	24.7%	6.4%
SIC > 90%	76.9%	83.2%	54.0%	12.0%	19.1%	31.1%	5.6%
SIC 10%–90%	84.2%	82.6%	54.3%	6.7%	37.3%	31.1%	3.5%
Open water	86.4%	84.0%	59.7%	3.8%	31.9%	26.0%	5.6%
Greenland	55.0%	74.8%	63.3%	28.4%	10.7%	14.9%	8.3%
Day	76.6%	79.9%	57.5%	10.1%	23.5%	25.5%	6.6%
Night	66.1%	71.5%	56.9%	14.2%	17.5%	20.3%	5.7%
			Autumn				
Total	73.1%	85.5%	71.3%	17.8%	21.2%	16.0%	10.1%
SIC > 90%	60.9%	89.5%	74.3%	34.3%	19.5%	16.3%	14.6%
SIC 10%–90%	76.6%	93.5%	72.9%	21.4%	51.1%	20.2%	7.9%
Open water	90.0%	90.9%	77.5%	3.5%	24.2%	14.0%	11.4%
Greenland	58.5%	74.5%	60.3%	28.2%	25.0%	17.7%	6.5%
Day	80.9%	85.0%	69.4%	8.1%	21.0%	17.1%	9.3%
Night	69.2%	85.7%	72.2%	22.5%	21.4%	15.5%	10.5%

not as consistent with those of CPR and MODIS. For the entire Arctic MODIS cloud fraction differs most from CALIOP during winter (by 15.5% and a cloudy disagreement of 28%) and is most consistent with CALIOP during summer (by only 3.6% and a cloudy disagreement of 10.7%). Contrary to CALIOP and MODIS, the CPR cloud fraction is surprisingly lowest during summer at 57.3% with cloudy disagreement of 24.7%.

Low cloud fraction in the Arctic during the summer has been used to explain, in part, the large decline in the sea ice perennial ice cover in 2007 (Kay et al. 2008; Kay and Gettelman 2009). We estimated the cloud fraction in the Arctic study area (60°–82°N) using CALIOP during summer (June, July, and August) and found 78.4% in 2007, when the perennial ice had the record low extent, and 78.4% in 2010, when the perennial ice was on a slight recovery and significantly more extensive than in 2007. The difference in cloud fraction for these two years is considered insignificant. With MODIS the corresponding values for 2007 and 2010 are 74.8% and 74.9%, respectively—the difference of which is again insignificant. These results indicate that further studies are needed to establish the impact of clouds on the declining sea ice cover in the summer. To gain insights into why some clouds are not detected by the sensors, we discuss in the following section the characteristics of these undetected clouds.

d. Characteristics of clouds not detected by each sensor

The multisensor capability of the A-Train enables us to better understand why one of the sensors is sometimes

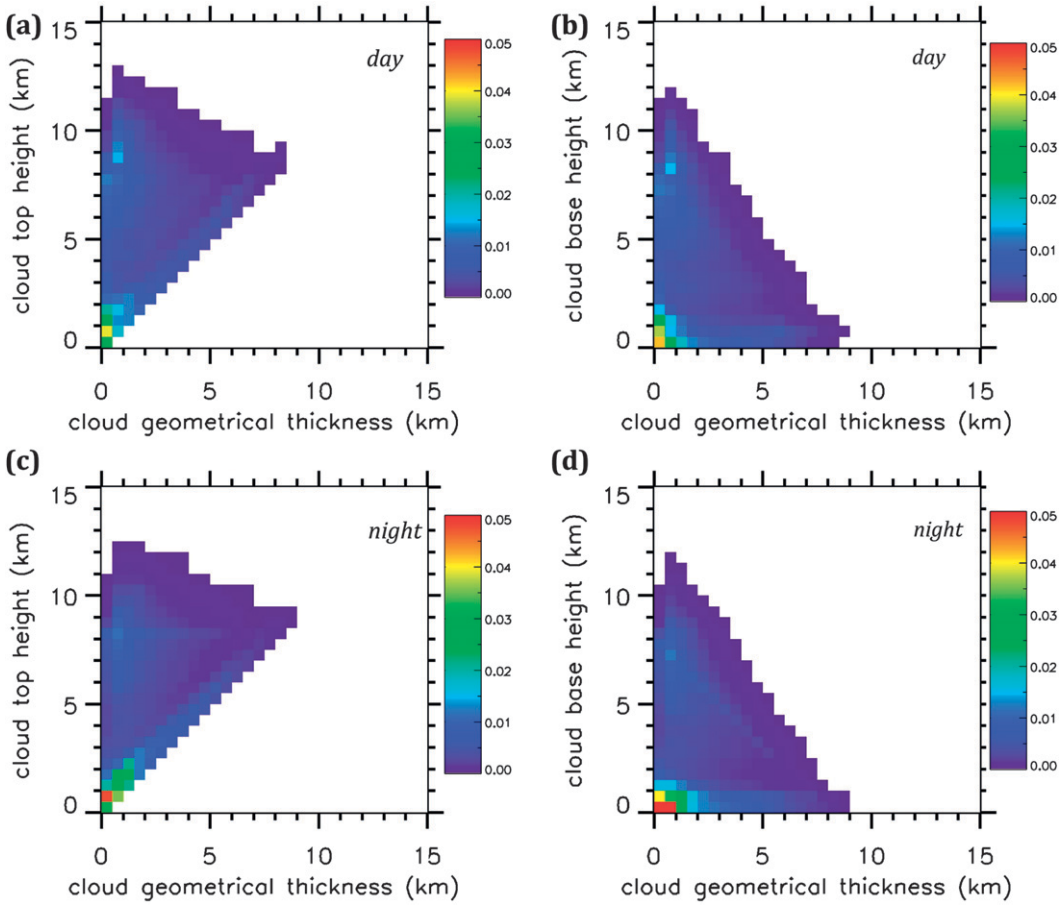

FIG. 9. Characteristics of Arctic clouds (60°–82.5°N) not detected by MODIS as determined by CALIOP. Two-dimensional histograms of CTH/CBH against geometrical thickness of clouds for (a),(b) daytime and (c),(d) nighttime conditions. Values are presented as a fraction of the total number of occurrences.

unable to detect the presence of clouds. The basic parameters are cloud-top height (CTH), cloud-base height (CBH), and cloud thickness (CT), all derived from CALIOP and/or CPR but used in the analysis of cloud data from all three sensors. We have presented individual cases in Figs. 1–6 but, in this section, provide more comprehensive statistics for the pan-Arctic region. In Fig. 9, we show frequency of occurrence histograms of CTH and CBH plotted versus CT for the special cases where clouds are not detected by MODIS, but are detected by CALIOP. The histograms were done separately for daytime (Figs. 9a and 9b) and nighttime cases (Figs. 9c and 9d) since the statistics are very different for the two cases. The color of a pixel represents a fraction of the total number of MODIS nondetections. In Fig. 9a, the histogram shows that MODIS cannot detect a wide range of cloud types from low-level clouds, thin cirrus, and even geometrically thick/convective clouds. Similarly, during nighttime the histogram has an ''inverted triangle'' shape, as shown in Fig. 9c. There is an increase in the nondetection of low-level clouds (CTH $<$ 2.5 km). In fact, the nondetection rate of low-level clouds increases from 24.7% during daytime to 31.7% during nighttime. This is likely the cause of the higher disagreement between CALIOP and MODIS during nighttime than daytime, as shown in Table 1. Both daytime and nighttime histograms of cloud-base height depict an ''upright triangular'' pattern, as shown in Figs. 9b and 9d, This means that the MODIS cloud mask misses clouds adjacent to the surface even if these are geometrically thick. These clouds can have thicknesses ranging up to 9 km, but at higher cloud-base height altitudes, this range narrows down to geometrically thinner clouds. As shown in Fig. 9b, a high number of undetected clouds in MODIS occurs for low-level clouds (CBH $<$ 2 km) with geometrical thickness ($<$2 km). This 2 km by 2 km ''blind box'' accounts for about 25.6% of all the clouds missed by MODIS. At higher altitudes, midlevel

clouds (CBH 2–6 km) are mostly identified by MODIS and thin, high-level clouds (CBH > 6 km) are more problematic, as suggested by the increased color intensity over the region. MODIS cloud detection is also influenced by optical thickness. Geometrically thick clouds may be optically thin, which causes them to be not detected by MODIS; on the other hand, optically and geometrically thick clouds have high reflectance similar to that from snow-covered/ice sheet surfaces.

For nighttime MODIS cloud detection, the general characteristics of the histogram are similar to that for daytime, having the same triangular pattern. However, there is a subtle broadening of the upright triangular pattern and an increase in the values of the 2 km by 2 km blind box to as high as 33.5%. This means that the transition to nighttime cloud detection causes MODIS to miss geometrically thicker clouds at all altitude levels and that it becomes difficult to detect thin, low-level clouds.

To present a better quantification of the differences between daytime and nighttime cloud detection performance of MODIS, Fig. 10 provides histograms of cloud-top height and thickness of clouds missed by MODIS over the entire Arctic (60°–82.5°N), with a division between nighttime and daytime detection. As shown in Fig. 10a, it is evident that the highest MODIS nondetection rates are for very low clouds and high clouds, as seen from the two distinct peaks in the histogram, and the peaks are more distinct for nighttime cases. In contrast, the histogram for cloud geometrical thickness, shown in Fig. 10b, has a decreasing trend as cloud geometrical thickness increases. In fact, geometrically thin clouds (<2 km) contribute to as much as 64.5% of the clouds not detected by MODIS. Because of proximity to the surface, thin low-level clouds could have nearly similar temperature as the underlying surface while the thin, high-level clouds have low temperatures comparable to those of sea ice or ice sheet. This, in turn, limits the infrared contrast between clouds and the background surface, causing the MODIS cloud detection algorithm to erroneously identify these cloud types as clear sky observations instead. It is also apparent that a large part of the undetected clouds comes from nighttime scenes, as indicated by the much larger bar stacked on the daytime values, consistent with the data in Table 1.

Figures 10c and 10d show histograms of cloud properties for undetected clouds over sea ice regions (>90% concentration). The frequency distribution of cloud-top heights over sea ice shown in Fig. 10c has two peaks located at 0.5–1.0 km and 8.0–8.5 km. These peaks are sharp and are only limited to a single 0.5-km bin. Mid-level clouds show a near-constant number of nondetection occurrences, and finally the nondetection rate of high clouds starting from a CTH of 8 km declines rapidly. The peaks occur during nighttime, when the uncertainties in cloud detection are large, and they might be caused in part by the limited thermal contrast between the surface and the high (or low) clouds. The peak at higher altitudes means that cloud temperatures at higher altitudes are similar to those over the sea ice surface, and this is possible due to frequent atmospheric inversions over the Arctic. The frequency distribution of the cloud geometrical thickness shown in Fig. 10d is similar to Fig. 10b. That is, geometrically thinner clouds are much more difficult to detect. As shown in Fig. 10e, for cases over open waters the cloud detection capabilities of MODIS substantially improve, as it detects most of the midlevel and high-level clouds (>3 km). The better thermal and visible contrast between clouds and open waters leads to the improvement in the accuracy of MODIS cloud detection. Furthermore, as shown in Fig. 10f, geometrically thicker clouds (>3 km) can be detected most of the time, with only 16.9% labeled clear by MODIS.

Over Greenland the number of daytime clouds not detected by MODIS is nearly the same as that for nighttime. This is evident as the lengths of the bar (representing number of occurrences) corresponding to nighttime and daytime are nearly identical, as shown in Fig. 10g. It is interesting that the performance of the MODIS cloud-masking algorithm is similar for both daytime and nighttime conditions. This is, in part, because the algorithm does not utilize any of the visible channels for surface elevations over 2 km. Also, the low water vapor conditions make cirrus clouds hardly discernible using the 1.38-μm water vapor channel as the surface radiative contribution on the signal is enhanced, making the visible identification tests ineffective. Cloud-top height distribution is similar to the case for all of the Arctic in Fig. 10a, but with fewer instances of nondetection for low clouds (CTH < 1 km) since most of the ice sheet is at an elevation higher than 1 km. As shown in Fig. 10h, the frequency distribution of cloud geometrical thickness increases as cloud thickness shrinks.

The characteristics of clouds that CPR cannot detect are distinctly different from that of MODIS. As shown in Fig. 11a, the histogram does not have the triangular pattern, and nondetection instances are limited to geometrically thinner clouds (<2.5 km). There is also a high concentration of CPR cloud nondetections for very low clouds with base heights below 1 km and geometrical thicknesses less than 1 km (a CPR 1 km by 1 km blind box), which amounts to about 53.2% of all clouds missed by CPR. Figure 11b further confirms that CPR is basically ''blind'' to very low clouds (CTH < 1 km) and that its cloud detection performance improves for mid-level clouds (CTH between 2 and 5 km) before finally

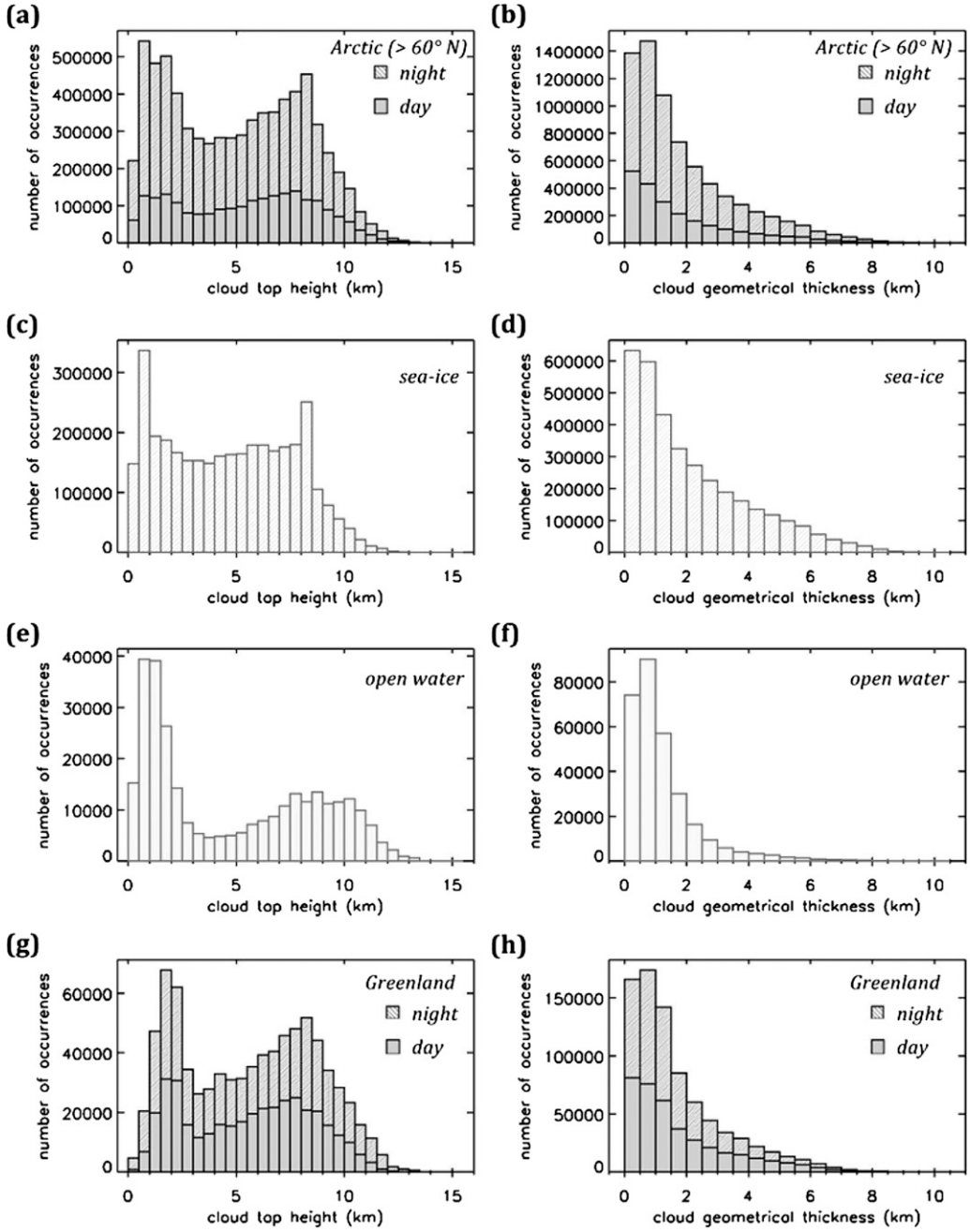

FIG. 10. Characteristics of clouds not detected by MODIS over different surface types and solar conditions. Combined night (black) and day (blue) histograms of (a) cloud-top height and (b) cloud geometrical thickness. Cloud property histograms for cases over (c),(d) sea ice, (e),(f) open waters, and (g),(h) Greenland (for ice sheet surfaces ≥2 km).

increasing again for high-level clouds (CTH > 6 km), thus creating another peak. Figure 11c shows that a large fraction of the clouds not detected by CPR (95.5%) corresponds to geometrically thin clouds (<2 km).

CALIOP cloud detection is superior compared to that from MODIS and CPR and is able to detect clouds with optical thickness as low as 0.01 (McGill et al. 2007). However, there are instances wherein MODIS detects a cloud feature that is missed by CPR and misclassified by CALIOP (Chan and Comiso 2011, and Fig. 6). For scenes with solar illumination, MODIS is able to effectively detect these specific types of clouds using the

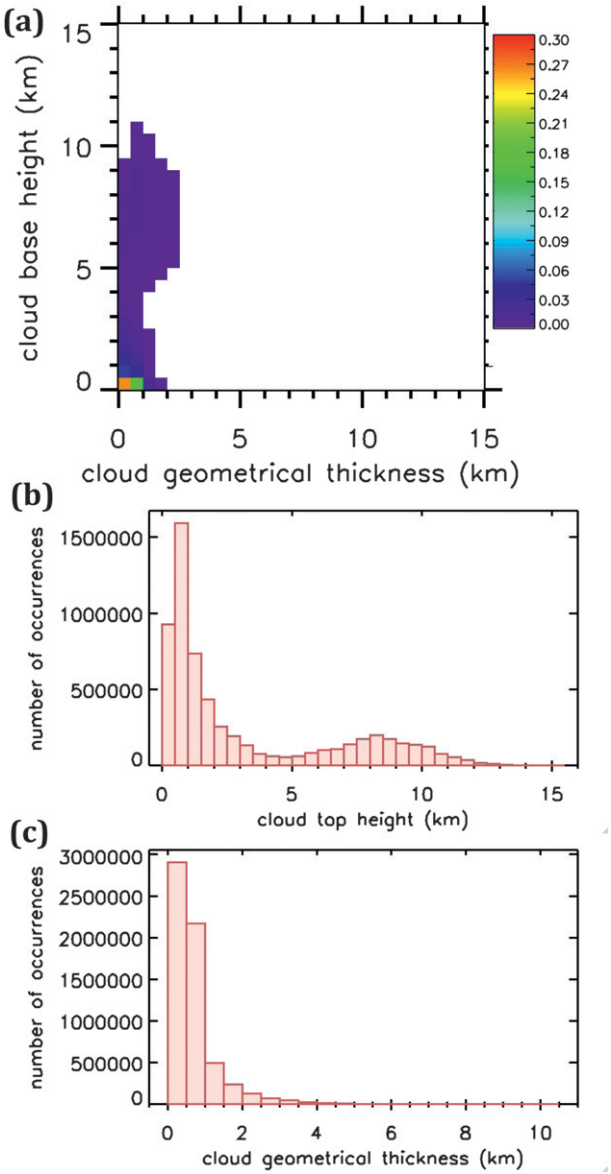

FIG. 11. (a) Two-dimensional histogram of cloud geometrical thicknesses and base heights of clouds not detected by CPR as determined from CS-GEOPROF-lidar; (b) CBH and (c) geometrical thickness histograms of clouds missed by CPR.

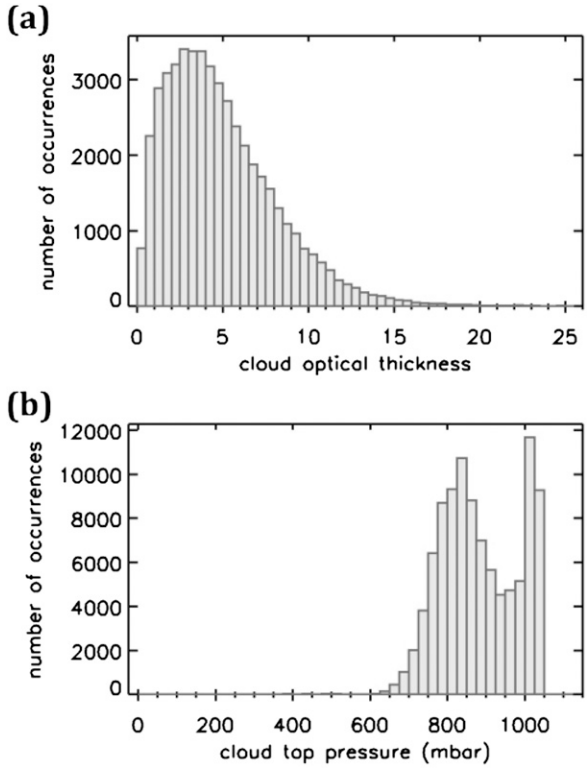

FIG. 12. Histograms of (a) cloud optical thickness and (b) cloud-top pressure for clouds not detected by either CALIOP or CPR but detected by MODIS (daytime over open waters from 60° to 82.5°N).

shortwave infrared channels (e.g., 3.75 μm) or visible channels (e.g., 0.87 μm). Figure 12a shows a histogram of cloud optical thickness retrieved by MODIS for cases where CALIOP and CPR miss clouds over open water. It can be observed that there is a wide range of optical thicknesses up to 18 and that the average optical thickness is 5. It should be noted that these values of optical thickness are well within the measurement capabilities of CALIOP, and such clouds can deliver a detectable backscatter signal. As shown in Fig. 12b, the MODIS-derived cloud-top pressure distribution of these undetected clouds is in a high pressure region greater than 700 hPa, and the average cloud-top pressure is 870 hPa. The optical thickness and the cloud-top pressure values of these clouds are comparable to the properties of marine stratus from Dong et al. (2001) and Chang and Coakley (2007). This suggests that those clouds not detected by CALIOP and CPR are actually low-level marine stratus.

4. Conclusions

A comprehensive study of the general characteristics of the cloud cover in the Arctic has been conducted using 2007 and 2010 data from *Aqua*/MODIS, *CALIPSO*, and *CloudSat*, all of which are in the A-Train. The results show a generally cloudy Arctic, especially in the ice-free ocean regions. The capabilities of the three sensors at detecting the cloud cover in the region were also studied and compared. Although the spatial distributions of clouds as detected by the three sensors are generally consistent, we find several cases in which there are significant discrepancies. For example, there are times when

cloud features that are apparent in the MODIS visible channel and also evident in the CALIOP and CPR data are identified by the MODIS cloud mask algorithm as cloud-free. There are also times when clear scenes as detected by CALIOP, CPR, and MODIS visible channel are identified by the MODIS cloud mask algorithm as cloudy. Furthermore, there are cases when CALIOP and CPR are not able to detect clouds that are easily identifiable in the MODIS visible channel.

To assess the importance of the observed inconsistencies in the detection of clouds, synoptic cloud fractions over the Arctic during the months of February (near sea ice maximum) and September (sea ice minimum) from the three instruments were presented. With CALIOP as the baseline, MODIS cloud map shows that there is a large negative bias in cloud cover over sea ice and positive bias over open waters. MODIS cloud fraction bias over sea ice tends to be larger in magnitude during February than September, mainly because of the lack of solar illumination. Conversely, MODIS cloud fraction has a larger positive bias over open waters for the month of September than for February. CPR cloud fractions consistently underestimate cloud cover across various surface types compared to the other sensors, with the exception for February, when MODIS cloud fraction over sea ice is lower than that from CPR. Moreover, the negative cloud fraction bias from CPR is worse during September compared to that for February (opposite behavior compared to MODIS).

To gain insights into the accuracy of the retrievals, we evaluated the statistical frequency of detection, and determined potential reasons for the discrepancies, using data from the three sensors for the entire year of 2007 and 2010. We found that, overall, the annual averages of cloud cover in the Arctic region are 66.8%, 78.4%, and 63.3% as inferred from MODIS, CALIOP, and CPR, respectively. We also found that the discrepancies were different for various surface types, for day versus night, and for different seasons.

For the entire Arctic, the disagreement between MODIS and CALIOP increased from 12.5% during daytime to 28.2% during nighttime. During nighttime, the magnitude of the bias is higher because cloud detection is limited to infrared bands owing to the lack of solar illumination. Seasonal cloud variations from the three sensors do not agree in terms of trend, magnitude, and occurrence of cloud cover maximum and minimum. Overall, the cloud detection performance of MODIS is best during summer and worst during winter, and it is highly dependent on surface type and solar illumination. As observed, the MODIS and CALIOP cloudy percentage disagreements over sea ice, Greenland, and Arctic nighttime are very high at 30.9%, 31.5%, and 26.7%, respectively. However, for sunlit conditions and open water, MODIS and CALIOP disagreements are less at 13.1% and 3.75%, respectively. MODIS/CALIOP clear sky percentage disagreement over open water is at 28.2%, with MODIS overestimating cloud cover in open water regions. On the other hand, CPR and CALIOP overall cloudy and clear sky percentage differences are 19.1% and 9.7%, respectively. CPR cloud detection is not directly affected by changes in the surface and solar conditions but, rather, by the prevalence of the types of clouds that it misses (e.g., diurnal variation of cloud characteristics). The characteristics of clouds missed by MODIS can have diverse properties that sometimes include geometrically thick clouds up to 8 km thick. MODIS nighttime cloud detection suffers because of the lack of thermal contrast between low-level clouds or high-level clouds (during thermal inversions) against the background surface. On the other hand, CPR misses much of the clouds with base height below 1 km that have geometrically thin features (<1 km). It is also evident that CPR frequently misses thin (<2.5 km) clouds at high altitude (6–10 km). Lastly, there are also cases where neither CALIOP nor CPR detects a cloud observed by MODIS, such as low-level marine stratus with an average optical thickness of 5 and cloud-top pressure greater than 870 hPa.

The results of this study indicate shortcomings in the archived cloud products from the three sensors—of which users should be aware. The MODIS cloud cover information is usually most desirable because the sensor is an imager and the data provide good temporal and spatial resolution. The inability of MODIS to identify cloud features consistently is unfortunate, and data use needs to be examined in the context of associated errors when utilized for climate modeling and radiative transfer studies. Also, there are currently several surface parameters that are derived from MODIS, and the accuracies of these parameters need to be reevaluated with the impact of the observed errors in cloud masking taken into consideration. Our study indicates that the CALIOP sensor provides highly accurate observation of clouds except in cases when the cloud is close to the surface and is geometrically thin. CPR also provides useful information of cloud thickness, but it is not as dependable as CALIOP in identifying clouds. Because of the importance of the MODIS cloud data, future work should include the development of a more accurate cloud masking algorithm for MODIS. In this endeavor, a technique that utilizes the concurrent use of CALIOP and CPR data will be very useful.

Acknowledgments. We thank the MODIS, *CloudSat*, *CALIPSO*, and AMSR-E science teams for providing

excellent and accessible data products that made this study possible. These data were obtained from the National Snow and Ice Data Center (http://nsidc.org), the NASA Langley Research Center Atmospheric Science Data Center (http://eosweb.larc.nasa.gov/), the NASA LAADS Web (http://ladsweb.nascom.nasa.gov/), and the *CloudSat* data processing center (http://cloudsat.cira.colostate.edu/). The NASA Cryospheric Sciences program in part funds this project.

REFERENCES

Ackerman, S. A., K. I. Strabala, W. P. Menzel, R. A. Frey, C. C. Moeller, and L. E. Gumley, 1998: Discriminating clear-sky from clouds with MODIS. *J. Geophys. Res.,* **103** (D24), 32 141–32 157.

Chan, M. A., and J. C. Comiso, 2011: Cloud features detected by MODIS but not by *CloudSat* and CALIOP. *Geophys. Res. Lett.,* **38,** L24813, doi:10.1029/2011GL050063.

Chang, F. L., and J. A. Coakley Jr., 2007: Relationship between marine stratus cloud optical depth and temperature: Inferences from AVHRR observations. *J. Climate,* **20,** 2022–2036.

Comiso, J. C., 2012: Large decadal decline of the Arctic multiyear ice cover. *J. Climate,* **25,** 1176–1193.

——, D. J. Cavalieri, and T. Markus, 2003: Sea ice concentration, ice temperature, and snow depth using AMSR-E data. *IEEE Trans. Geosci. Remote Sens.,* **41,** 243–252.

——, C. L. Parkinson, R. Gersten, and L. Stock, 2008: Accelerated decline in the Arctic sea ice cover. *Geophys. Res. Lett.,* **35,** L01703, doi:10.1029/2007GL031972.

Curry, J. A., W. B. Rossow, D. Randall, and J. L. Schramm, 1996: Overview of Arctic cloud and radiation characteristics. *J. Climate,* **9,** 1731–1764.

Dong, X., G. G. Mace, P. Minnis, and D. F. Young, 2001: Arctic stratus cloud properties and their effect on the surface radiation budget: Selected case from FIRE ACE. *J. Geophys. Res.,* **106** (D14), 15 297–15 312.

——, B. Xi, K. Crosby, C. N. Long, R. S. Stone, and M. D. Shupe, 2010: A 10 year climatology of Arctic cloud fraction and radiative forcing at Barrow, Alaska. *J. Geophys. Res.,* **115,** D17212, doi:10.1029/2009JD013489.

Francis, J. A., and E. Hunter, 2006: New insight into the disappearing Arctic sea ice. *Eos, Trans. Amer. Geophys. Union,* **87,** 509–511.

Frey, R. A., S. A. Ackerman, Y. Liu, K. I. Strabala, H. Zhang, J. R. Key, and X. Wang, 2008: Cloud detection with MODIS. Part I: Improvements in the MODIS cloud mask for collection 5. *J. Atmos. Oceanic Technol.,* **25**, 1057–1072.

Holland, M. M., and C. M. Bitz, 2003: Polar amplification of climate change in coupled models. *Climate Dyn.,* **21,** 221–232.

Holz, R. E., S. A. Ackerman, F. W. Nagle, R. Frey, S. Dutcher, R. E. Kuehn, M. A. Vaughan, and B. Baum, 2008: Global Moderate Resolution Imaging Spectroradiometer (MODIS) cloud detection and height evaluation using CALIOP. *J. Geophys. Res.,* **113,** D00A19, doi:10.1029/2008JD009837.

Hu, Y., and Coauthors, 2009: *CALIPSO*/CALIOP cloud phase discrimination algorithm. *J. Atmos. Oceanic Technol.,* **26,** 2293–2309.

Karlsson, K. G., and A. Dybbroe, 2010: Evaluation of Arctic cloud products from the EUMETSAT Climate Monitoring Satellite Application Facility based on *CALIPSO*–CALIOP observations. *Atmos. Chem. Phys.,* **10,** 1789–1807.

Kay, J. E., and A. Gettelman, 2009: Cloud influence on and response to seasonal Arctic sea ice loss. *J. Geophys. Res.,* **114,** D18204, doi:10.1029/2009JD011773.

——, T. L'Ecuyer, A. Gettelman, G. Stephens, and C. O'Dell, 2008: The contribution of cloud and radiation anomalies to the 2007 Arctic sea ice extend minimum. *Geophys. Res. Lett.,* **35,** L08503, doi:10.1029/2008GL033451.

Kellogg, W. W., 1975: Climate feedback mechanisms involving the polar regions. *Climate of the Arctic,* G. Weller and S. A. Bowling, Eds., Geophysical Institute, University of Alaska, 111–116.

Liu, Y., S. A. Ackerman, B. C. Maddux, J. R. Key, and R. A. Frey, 2010: Errors in cloud detection over the Arctic and implications for observing feedback mechanisms. *J. Climate,* **23,** 1894–1907.

Liu, Z., and Coauthors, 2009: The *CALIPSO* lidar cloud and aerosol discrimination: Version 2 algorithm and initial assessment of performance. *J. Atmos. Oceanic Technol.,* **26,** 1198–1213.

Marchand, R., G. G. Mace, T. Ackerman, and G. Stephens, 2008: Hydrometeor detection using *Cloudsat*—An earth-orbiting 94-GHz cloud radar. *J. Atmos. Oceanic Technol.,* **25,** 519–533.

McGill, M. J., M. A. Vaughan, C. R. Trepte, W. D. Hart, D. L. Hlavka, D. M. Winker, and R. Kuehn, 2007: Airborne validation of spatial properties measured by the *CALIPSO* lidar. *J. Geophys. Res.,* **112,** D20201, doi:10.1029/2007JD008768.

Schweiger, A. J., R. W. Lindsay, S. Vavrus, and J. A. Francis, 2008: Relationship between Arctic sea ice and clouds during autumn. *J. Climate,* **21,** 4799–4810.

Stephens, G. L., and Coauthors, 2002: The *CloudSat* mission and the A-Train: A new dimension of space-based observations of clouds and precipitation. *Bull. Amer. Meteor. Soc.,* **83,** 1771–1790.

Wang, C., Z. J. Luo, and X. Huang, 2011: Parallax correction in collocating *CloudSat* and Moderate Resolution Imaging Spectroradiometer (MODIS) observations: Methods and application to convection study. *J. Geophys. Res.,* **116,** D17201, doi:10.1029/2011JD016097.

Wang, X., and J. R. Key, 2005: Arctic surface, cloud, and radiation properties based on the AVHRR Polar Pathfinder dataset. Part I: Spatial and temporal characteristics. *J. Climate,* **18,** 2558–2574.